Colloid Polym Sci (2015) 293:2469–2475
DOI 10.1007/s00396-015-3639-z

ORIGINAL CONTRIBUTION

The impact of *trans*/*cis* photoisomerization on photoinduced electron transport between 4,4′-stilbenedicarboxylic acid and columnar perylenediimide aggregates in water

Ruimin Zhu[1] · **Yingyuan Zhao**[1] · **Tingting Sun**[1] · **Heyuan Liu**[1] · **Ying Zhang**[1] · **Xiyou Li**[1]

Received: 5 April 2015 / Accepted: 26 May 2015 / Published online: 5 June 2015

Abstract Photoinduced electron transfer (PET) between self-assembled *trans*- or *cis*-isomer of 4,4′-stilbenedicarboxylic acid (SDBA) and [*N*,*N*′-di(2-(trimethylammoniumiodide)ethylene)]perylenediimide (PDI-I) in water has been investigated. Both *trans*-SDBA and *cis*-SDBA molecules can form stable complexes with columnar PDI-I aggregates in water with a 1:1 stoichiometry via ionic interactions, but the complex of *cis*-isomer is more stable as revealed by the UV-vis absorption and fluorescence spectroscopy. The electrochemical experiments suggest that *cis*-SDBA is a better electron donor than its *trans*-isomer. However, fluorescence quenching experiments suggest that the electron transfer from *trans*-SDBA is more efficient than that from *cis*-SDBA, which is obviously contradictory to the results of binding constant and the electrochemical experiments. The contradictory results can be attributed to that the columnar aggregates $(PDI\text{-}I)_n$ are utterly destroyed in *cis*-SDBA-$(PDI\text{-}I)_n$ system caused by stronger ionic interaction between *cis*-SDBA and $(PDI\text{-}I)_n$. Also, the bending conformation of *cis*-SDBA probably results in a larger distance between *cis*-SDBA and the surface of $(PDI\text{-}I)_n$. The results of this research suggest that the electron transfer can be tuned by the aggregation and/or configuration of the donors and acceptors.

Electronic supplementary material The online version of this article (doi:10.1007/s00396-015-3639-z) contains supplementary material, which is available to authorized users.

✉ Xiyou Li
xiyouli@sdu.edu.cn

[1] Key Laboratory for Colloid and Interface Chemistry, Ministry of Education, Department of Chemistry, Shandong University, Jinan, Shandong, People's Republic of China

Keywords *Trans*/*cis* photoisomerization · Columnar perylenediimide aggregate · Photoinduced electron transfer · Fluorescence quench · Quantum yield

Introduction

Photoinduced electron transfer (PET) is an essential process in photosynthesis [1–3], which is also a fundamental process in solar cells [4, 5] and photodegradation of pollutants [6]. Many organic compounds with covalently linked donor and acceptor moiety have been designed and synthesized for the purpose of revealing the origin of PET process [7–9]. At the same time, mimicking the natural PET with non-covalently systems based on varies of supramolecular interactions has also gained much attention in the past several decades [10, 11]. In these supramolecular systems, electron donors and acceptors self-assemble into complexes, which offer the place for the PET process. Naturally, the rate and efficiency of PET process are determined by supramolecular interactions between donors and acceptors, such as weak intermolecular interactions [12–14] and/or hydrogen bonding [15] and/or ionic interactions [9], which affect the combination mode between donor and acceptor. Appropriate combination mode will result in effective overlap of the electron cloud between donor and acceptor and favor the PET process. As a matter of fact, the interaction modes are closely related to the structures of donors and acceptors [16]; therefore, the PET in a supramolecular system is determined by the structure of the donor and acceptor.

Perylenetetracarboxylic diimides (PDI) is a special class of n-type semiconductors and commonly used in optoelectronic devices owing to the outstanding photochemical and photophysical properties [17–19]. Especially, the one-

dimensional PDI assembly, which can provide a pathway for electron delocalization and have low reduction potential, is recognized as a good candidate of electron acceptors for PET process [20].

Stilbenes are a group of widely studied molecules in photochemistry, especially for 4,4′-stilbenedicarboxylic acid (SDBA) [21–25], due to their special photoisomerization [26–28] and [2+2] photocycloaddition [29] properties. From the perspective of PET process, SDBA molecules are good candidates as electron donors [30–32] and a good model to study isomerisation effect on PET.

In the present work, SDBA isomers were chosen as electron donors and PDI-I as electron acceptor in order to investigate the impact of *trans*/*cis* isomerization of SDBA on the PET between SDBA isomers and PDI aggregates. The structures of PDI-I and SDBA are shown in Scheme 1.

Experimental

Materials

PDI-I was synthesized according to the reported method [33], and the details were presented in the supplementary material. Purification of water was performed with a Molecule Lab Water Purifier (Gene 1810D), and the ultrapure water (>18.2 MΩ cm, 25 °C) was used in all experiments. *Trans*-SDBA was purchased from Alfa Aesar (96 %). *Cis*-SDBA was obtained from configuration transformation of *trans*-SDBA under the irradiation of Xe lamp (500 W, LSH-X500) with 310 nm optical filter [34].

Instruments and methods

^{1}H NMR spectra were recorded on a Bruker 400 MHz NMR spectrometer with chemical shifts reported in ppm (TMS as internal standard). Absorption spectra were measured on SHIMADZU UV-2450 spectrophotometer. Steady-state fluorescence spectra were recorded on F-280 fluorescence spectrophotometer. Fluorescence quantum yields were calculated with *N*,*N*′-di(octyl)-perylenediimide in chloroform as standard. Electrochemical measurements were carried out on CHI-760 electrochemical workstation in deaerated water containing 0.10 M Na_2SO_4 as supporting electrolyte. Typically, a conventional three-electrode cell was used with a platinum working electrode, a platinum wire as the counter electrode and a saturated calomel electrode (SCE) as reference electrode. The differential pulse voltammogram data was collected after N_2 purging into the solution for about 10 min. AFM images were obtained on Nanoscope (R) III with a tapping mode, and the samples were prepared on the quartz substrates. All the measurements were conducted at room temperature.

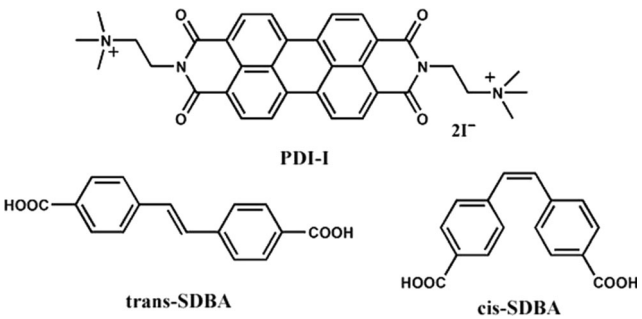

Scheme 1 Structures of PDI-I and SDBA isomers

Results and discussion

Photoisomerization of SDBA isomers

SDBA can dissolve freely in 0.01 M aqueous solution of KOH. The photoisomerization process from *trans*-SDBA to *cis*-SDBA was monitored by absorption spectroscopy. The absorption spectrum was collected for every 10-s illumination until the spectrum had no remarkable changes. As shown in Fig. 1, *trans*-SDBA presents absorption bands at 342, 326, and 313 nm. Under irradiation, the band intensities of these featured absorptions of *trans*-SDBA decrease, while the intensities of the featured bands of *cis*-SDBA at 302 and 235 nm [34] increase gradually. After irradiation for 30 s, the spectrum reaches a stable state and keeps unchanged under irradiation for even longer time (†Figure S1), indicating an equilibrium achieved for the photoisomerization. The fluorescence spectra of *trans*- and *cis*-SDBA are also distinctively different, as shown in Fig. 2. Although both *trans*- and *cis*-SDBA show emission band at 375 nm (λ_{ex}=300 nm), the fluorescence quantum yield of *cis*-SDBA (0.16) is significantly smaller than that of *trans*-SDBA (0.38), which is similar to other stilbenes [35].

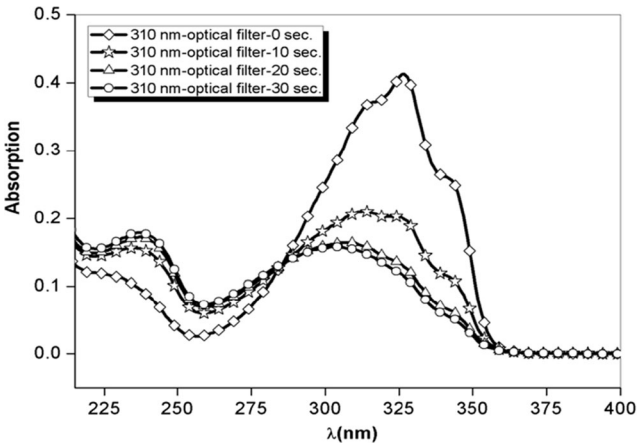

Fig. 1 Absorption spectrum of *trans*-SDBA (10^{-5} M) under the irradiation of Xe lamp with a 310-nm optical filter for every 10 s

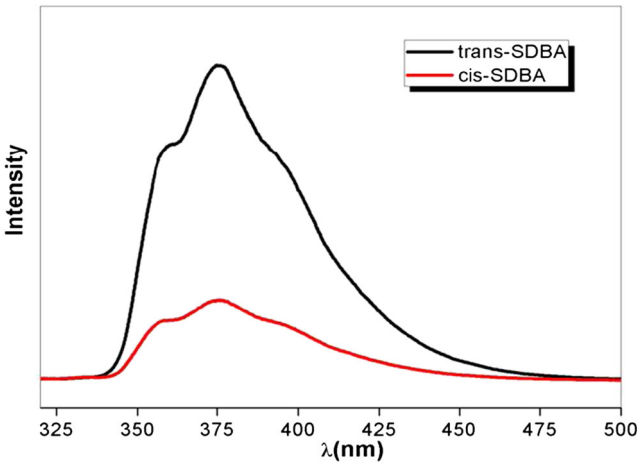

Fig. 2 Fluorescence spectra of *trans*- and *cis*-SDBA (10^{-5} M)

Formation of *trans*-SDBA-(PDI-I)$_n$ and *cis*-SDBA-(PDI-I)$_n$ complexes

Typically, PDI-I molecules self-assemble into aggregates (PDI-I)$_n$ in water with absorption bands at 534, 500, and 467 nm, which can be assigned to the 0-0, 0-1, and 0-2 vibronic bands of the first excited states, respectively [13]. Among these absorption bands, the 0-1 band has the largest intensity, which is a sign of the formation of "face-to-face" stacked PDI aggregates in solution [13, 20, 36]. The fluorescence spectrum of (PDI-I)$_n$ presents one broad band in the region of longer wavelength, which can be assigned to the "excimer-like" states due to the formation of "face-to-face" stacked structure [37, 38].

The formation of complexes between SDBA and (PDI-I)$_n$ induces large changes on both absorption and fluorescence spectra. As shown in Fig. 3a, along with the increase on the concentration of *trans*-SDBA in the aqueous solution of PDI-I, significant changes on the absorption spectrum of PDI-I can be found. The intensity of the absorption bands of PDI decreases gradually with the increasing amount of *trans*-SDBA [13]. No isosbestic point was observed during the titration. In addition, the absorption peaks of 0-0 and 0-1 bands of (PDI-I)$_n$ red-shift to 548 and 509 nm, respectively, demonstrating the presence of ionic interactions between *trans*-SDBA and (PDI-I)$_n$ and the absence of efficient π−π interactions between them [12]. It is also worth noting that the 0-1 vibronic band of PDI at about 500 nm is still the largest absorption band in the absorption spectrum of PDI-I in the presence of equivalence *trans*-SDBA, which means that the face-to-face stacked structure of (PDI-I)$_n$ is not broken utterly by the *trans*-SDBA molecules. As shown in Fig. 3b, fluorescence of (PDI-I)$_n$ is significantly quenched by *trans*-SDBA. The 1:1 stoichiometry between *trans*-SDBA and PDI-I was revealed by the plot of emission intensity at 548 nm vs the molar percentage of *trans*-SDBA in the mixture of SBDA and PDI-I as shown in the inset of Fig. 3b. The formation constant of the complex between *trans*-SDBA and (PDI-I)$_n$ deduced from the slope of the linear plot of $[\text{PDI-I}]_0/(I_0-I)$ vs $[\textit{trans}\text{-SDBA}]^{-1}$ at 550 nm is 1.3×10^4 M^{-1} (K_1) as shown by Fig. 3c [12].

The addition of *cis*-SDBA to the PDI-I solution also causes significant changes of the absorption of PDI-I, as shown in Fig. 4a, but the magnitude of the changes caused by *cis*-SDBA is obviously smaller than that caused by *trans*-SDBA. A few nanometer red-shifts are observed for 0-0 and 0-1 vibronic bands at 539 and 505 nm because of ionic interactions. There is also no isosbestic point in the absorption during the titration with *cis*-SDBA. The fluorescence of PDI-I was also quenched by *cis*-SDBA as shown in Fig. 4b. The plot of emission intensity at 548 nm vs the molar ratio of *cis*-SDBA in the mixture of *cis*-SDBA and PDI-I gives a break at 0.56, implying the 1:1 stoichiometry of the self-assembled complex. The decrease in fluorescence intensity at 548 nm provides a linear plot against the variation of reciprocal of *cis*-SDBA concentration (Fig. 4c), from which the formation constant of *cis*-SDBA-(PDI-I)$_n$ was obtained as 1.5×10^4 M^{-1} (K_2).

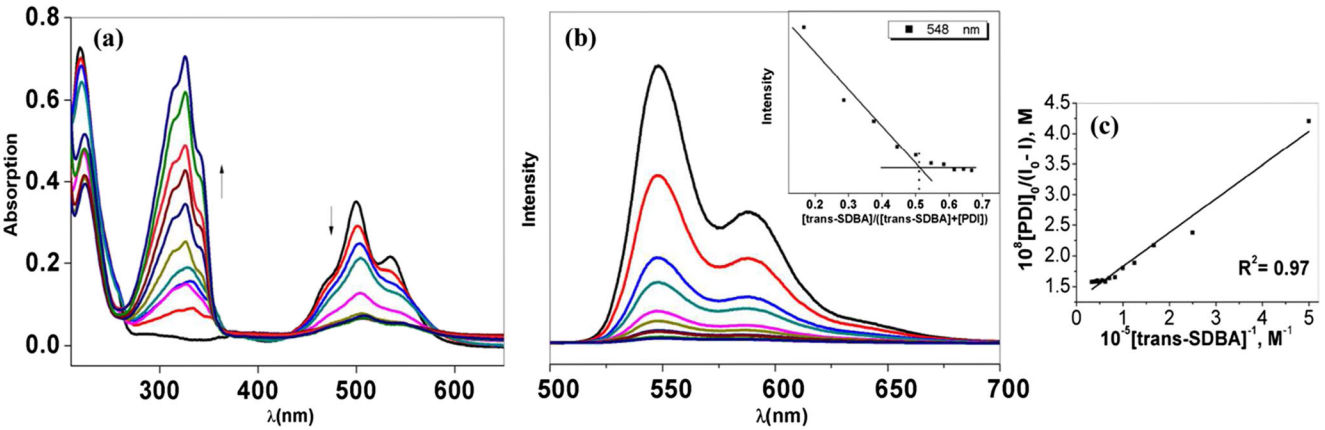

Fig. 3 **a** Uv-vis spectra of PDI in presence of increasing concentration (0~10^{-5} M) of *trans*-SDBA in water. **b** Corresponding fluorescence spectra after excluding the effect of absorption change at 450 nm.(λ_{ex}= 450 nm). *Inset*: plots of emission intensity I vs [*trans*-SDBA]/([*trans*-SDBA]+[PDI-I]). **c** Plots of $[\text{PDI}]_0/(I_0-I)$ vs $[\textit{trans}\text{-SDBA}]^{-1}$ at 550 nm

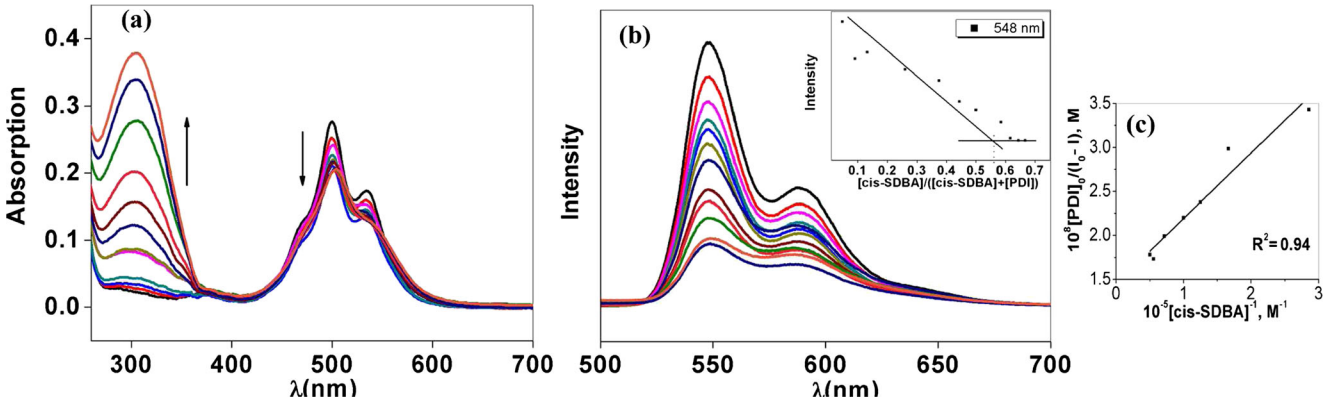

Fig. 4 **a** Uv-vis spectra of PDI in presence of increasing concentration (0~10^{-5} M) of *cis*-SDBA in water. **b** Corresponding fluorescence spectra after excluding effect of different absorptions at 450 nm.(λ_{ex}=450 nm). *Inset*: plots of emission intensity I vs [*cis*-SDBA]/([*cis*-SDBA]+[PDI-I]). **c** Plots of $[PDI]_0/(I_0-I)$ vs [*cis*-SDBA]$^{-1}$ at 550 nm

Apparently, K_2 is a little bit larger than K_1, indicating that ionic interactions between *cis*-SDBA and $(PDI\text{-}I)_n$ are larger than that between *trans*-SDBA and $(PDI\text{-}I)_n$. The stronger binding of *cis*-SDBA with PDI is probably caused by the alignment of the two carboxylic acid groups at the terminals of SDBA, which can be adsorbed simultaneously to the surface of cationic PDI aggregates without large steric hindrance.

Energetic of charge separation of *trans*-SDBA-$(PDI\text{-}I)_n$ and *cis*-SDBA-$(PDI\text{-}I)_n$

For the purpose of revealing the origin of the fluorescence quenching of PDI by SDBA, the redox potentials (E_{ox}) of *trans*-SDBA and *cis*-SDBA were determined by differential pulse voltammogram measurements in deaerated water with 0.10 M Na_2SO_4 as electrolyte (†Figure S2), and then, the free energies of photoinduced electron transfer (ΔG_{CS}) were calculated following Eq. 1 [39].

$$\Delta G_{cs} = e(E_{ox} - E_{red}) - \Delta E_s + \Delta G_s \quad (1)$$

$$\Delta G_s = 1.52(1/\varepsilon) - 0.064 \quad (2)$$

where E_{red} is the reduction potential of PDI-I in water, which was reported to be −0.25 V [13]. E_{ox} is the oxidation potential of SDBA in water. ΔE_s is the lowest singlet excited state energy of SDBA or PDI stacks, which can be calculated approximately by averaging the energies of corresponding (0-0) emission and (0-0) absorption band [14]. 3.54 eV for *trans*-SDBA, 3.78 eV for *cis*-SDBA, and 2.22 eV for PDI stacks were calculated. ΔG_s is the static Coulomb energy in water. The products of SDBA and $(PDI\text{-}I)_n$ aggregates in water are assumed to be solvent-separated ion pairs, so Eq. 2 is used to calculate ΔG_s, where ε is the dielectric constant of water [40].

The driving force (ΔG_{CS}) for the PET from *trans*-SDBA to $(PDI\text{-}I)_n$ column when SDBA was excited is estimated to be −2.5 eV, while that from *cis*-SDBA to PDI is −2.8 eV. Also, the driving forces (ΔG_{CS}) for the PET when PDI was excited are −1.14 and −1.18 eV for *trans*-SDBA and *cis*-SDBA, respectively. Therefore the PET process is a thermal dynamically favorable process in both systems, and the one from *cis*-SDBA to PDI is more energetically favorable. This result means that the fluorescence quenching of PDI caused by the PET from *cis*-SDBA should be more efficient.

Photoinduced electron transfer between SDBA isomers and columnar $(PDI\text{-}I)_n$

In order to evaluate the efficiency and rate constant of the fluorescence quenching of PDI-I by SDAB isomers, the fluorescence quantum yields of PDI-I in the presence of different concentrations of SDBA were measured, and the results are presented in Fig. 5a. The fluorescence quantum yields were calculated with [*N*,*N*-di(octyl)]perylenediimide in chloroform as standard. Along with the concentration increasing of *trans*-SDBA, the fluorescence quantum yield of PDI-I in aqueous solution decreases from 0.027 to 0.002, which means about 93 % of the fluorescence of $(PDI\text{-}I)_n$ is quenched by *trans*-SDBA. However, the same amount of *cis*-SDBA causes only 63 % fluorescence quenching of PDI-I. Apparently, *trans*-SDBA quenches the fluorescence of PDI-I aggregates more efficiently than *cis*-SDBA does in water.

Judging from the formation constants of the self-assembly and driving forces for the PET, *cis*-SDBA is a better electron donor than *trans*-SDBA. However, the results of fluorescence quantum yields and fluorescence quenching efficiencies suggest that the PET process goes more efficiently from *trans*-SDBA to $(PDI\text{-}I)_n$. To better understand these results, the following experiments were designed. Firstly, we had a hypothesis that the addition of *trans*- or *cis*-SDBA to the aqueous solution of PDI-I may affect the aggregation of PDI due to the strong ionic interactions [41] so that the charge-separated states cannot be stabilized significantly by the charge diffusion along the one-dimensional aggregates of PDI-I [42], which

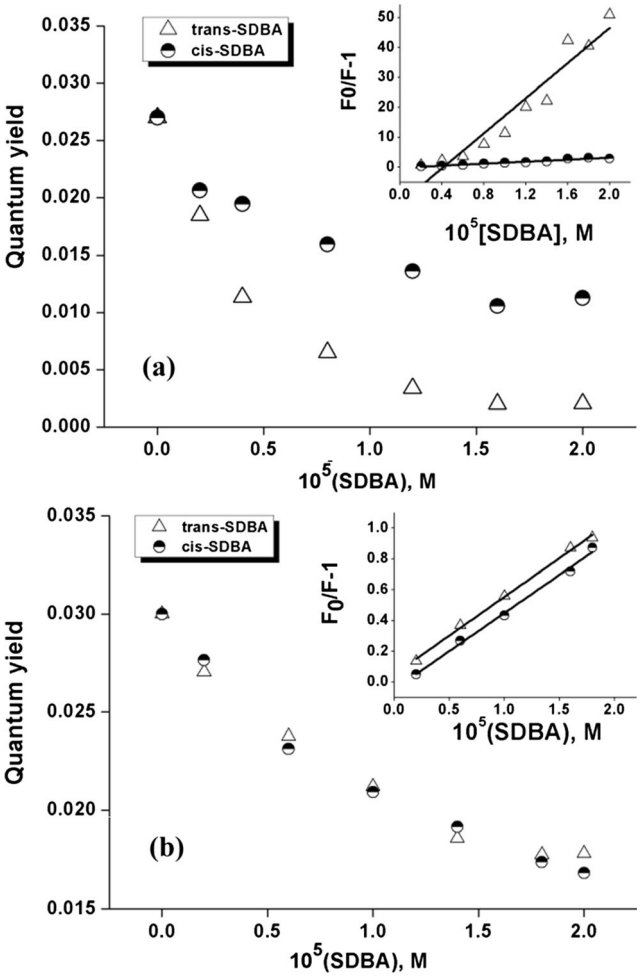

Fig. 5 Quantum yields of PDI-I in the presence of SDBA with increasing concentration. *Inset*: Stern-Volmer plot for PDI quenched by SDBA. **a** In water, **b** in methanol

reduce the actual driving force for the PET [43, 44]. Therefore, the similar fluorescence quenching experiments were carried out in methanol because PDI-I can be dissolved freely in methanol and no aggregates of PDI-I formed in methanol solution (†Figure S3). Apparently, the fluorescence quenching efficiency of PDI-I is approximately 44 % for *trans*-SDBA and 41 % for *cis*-SDBA with the same amount of quenchers, suggesting that the fluorescence quenching efficiencies of PDI-I by *trans*- and *cis*-SDBA are almost identical in methanol and both of them are smaller than that in water.

The results have also been confirmed by Stern-Volmer plots. In methanol, Stern-Volmer plots of *trans*-SDBA and *cis*-SDBA have good linearity with R^2=0.99, implying static quenching in both of them [44]. In aqueous solution, however, Stern-Volmer plot of *cis*-SDBA system shows adequate linearity with R^2=0.95, but Stern-Volmer plot of *trans*-SDBA system deviates slightly from linearity. Hence, static quenching occurs between $(PDI\text{-}I)_n$ and *cis*-SDBA, but dynamic and static quenching occurs simultaneously between $(PDI\text{-}I)_n$ and *trans*-SDBA in aqueous solution [45]. Moreover, the fluorescence quenching rate constants (K_{sv}) of PDI-I by two SDBA isomers in methanol are almost the same, but in aqueous solution, *trans*-SDBA presents larger quenching constant than *cis*-SDBA does.

For the further proof of our hypothesis, the morphologies of self-assembled *trans*-SDBA-$(PDI\text{-}I)_n$ and *cis*-SDBA-$(PDI\text{-}I)_n$ were examined by atomic force microscopy (AFM). The samples for the AFM examination were prepared by drop-casting corresponding solutions on Quartz wafer and evaporating gradually at room temperature. The resulted AFM images are shown in Fig. 6. Without *trans*- and *cis*-SDBA, PDI-I molecules self-assemble into one-dimensional nanocolumns with the length of several micrometers and the average width of 200 nm, which is consistent with the reported result [37] (Fig. 6a). After the addition of 0.5 equivalence of *trans*-SDBA, smaller nanocolumns with the length of less than micrometers and nanoparticles can be identified in the image (Fig. 6b). By contrast, the addition of *cis*-SDBA results in small nanoparticles of PDI-I (Fig. 6c). The

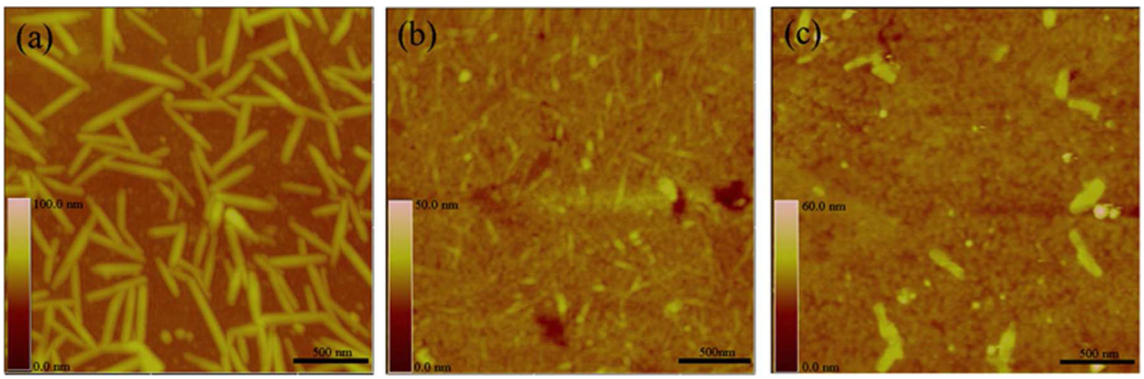

Fig. 6 AFM images of columnar $(PDI\text{-}I)_n$ and two ionic self-assembled SDBA-$(PDI\text{-}I)_n$ systems: **a** one-dimension nanostructures of PDI-I obtained from the aqueous solution (0.1 mM). **b** Nanostructures from 1:2 molar ratio of *trans*-SDBA vs PDI-I solution (0.1 mM). **c** Nanostructures from 1:2 molar ratio of *cis*-SDBA vs PDI-I solution (0.1 mM)

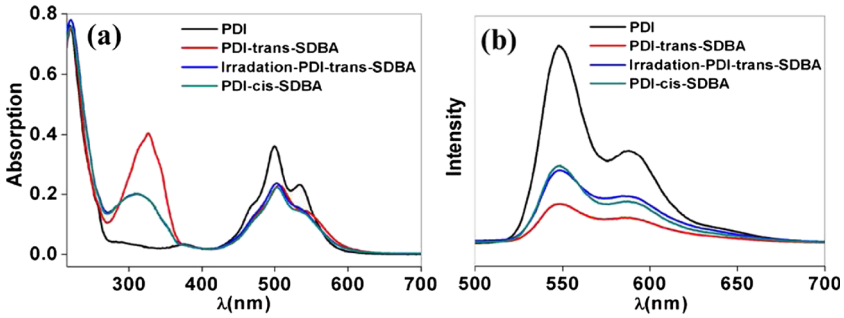

Fig. 7 **a** Uv-vis spectra of transformation of *trans*-SDBA-$(PDI-I)_n$ into *cis*-SDBA-$(PDI-I)_n$ (*trans*-SDBA:PDI-I=1:1). **b** Emission spectra of transformation of *trans*-SDBA-$(PDI-I)_n$ into *cis*-SDBA-$(PDI-I)_n$ system

linear aggregates were totally destroyed. Therefore both *trans*- and *cis*-SDBA can destroy the columnar $(PDI-I)_n$ aggregates, but the *cis* isomer seems more destructive as shown by the AFM images. So both the results of quenching experiment in methanol and AFM images agree well with our hypothesis.

Probable combination models for *trans*-SDBA-$(PDI-I)_n$ and *cis*-SDBA-$(PDI-I)_n$

The SDBA molecules can either adsorb on the surface of the column PDI-I aggregates or insert deeply into the column structure of the PDI-I aggregates. Theoretically, if the SDBA molecules were on the surface of PDI-I aggregates, the photoinduced isomerization from *trans*- to *cis*- should not be affected. Otherwise, the isomerization should be hammered by the rigid environment [46]. With this in mind, we tested the photo-driven isomerization of *trans*-SDBA to *cis*-SDBA in the presence of PDI-I aggregates, and the results are shown in Fig. 7a, b. After irradiation, the absorption in the range of 420–630 nm corresponding to the absorption of PDI-I aggregates keeps unchanged, but the absorption of *trans*-SDBA at 326 nm decreases and blue-shifts to 313 nm, which agrees very well with the absorption of *cis*-SDBA in the presence of PDI-I. In another word, *trans*-SDBA-$(PDI-I)_n$ can be transformed into *cis*-SDBA-$(PDI-I)_n$ easily and the isomerization rate is also not affected by the presence of $(PDI-I)_n$. Based on this result, we can concluded that both *trans*-SDBA and *cis*-SDBA molecules are probably adsorbed similarly on the surface of columnar PDI aggregates. However, because of the linear configuration of *trans*-SDBA, larger repulsion caused by the steric hindrance occurs between *trans*-SDBA molecules and the surface of PDI-I columns. By contrast, for *cis*-SDBA with the bending configuration, it allows anions and cations to come closely, which leads to a more stable binding between *cis*-SDBA molecules on the surface of PDI-I column. This is why the linear aggregates of PDI-I can only be partially destroyed by the *trans*-SDBA, but destroyed almost completely by the *cis*-isomer. Moreover, the bending configuration of *cis*-SDBA leads to a larger distance between *cis*-SDBA molecules and the surface of $(PDI-I)_n$, and then a slower PET between SDBA and PDI-I.

Conclusions

The columnar $(PDI-I)_n$ stacks can host *trans*- and *cis*-SDBA via ionic interactions in water. The strength of the interactions between *trans*-SDBA and $(PDI-I)_n$ are smaller than that between *cis*-SDBA and $(PDI-I)_n$ because the *trans* conformation leads to larger steric repulsion between SDBA molecules and $(PDI-I)_n$. The electrochemical studies revealed that *cis*-SDBA can provide electron more easily so it is a better electron donor than its *trans* isomer. However, the fluorescence quenching experiments suggest that the *trans*-SDBA is a better fluorescence quencher, in another word, the PET from *trans*-SDBA to $(PDI-I)_n$ is more efficient. These contradictory results can be attributed to that the columnar $(PDI-I)_n$ aggregates are almost utterly destroyed by *cis*-SDBA due to the stronger ionic interaction between *cis*-SDBA and $(PDI-I)_n$. Moreover, the bending configuration of *cis*-SDBA probably leads to a larger distance between the $(PDI-I)_n$ surface and *cis*-SDBA and thus a less efficient PET. So one can control the PET process by changing the configuration of donors and the aggregation properties of the acceptors, which is meaningful for the design of new optoelectronic devices.

References

1. Wasielewski MR (2006) J Org Chem 71:5051
2. Dutta PK (2011) J Phys Chem Lett 2:467
3. Sang L, Zhao Y, Burda C (2014) Chem Rev 114:9283
4. Kamat PV (2007) J Phys Chem C 111:2834
5. Listorti A, O' Regan B, Durrant JR (2011) Chem Mater 23:3381
6. Kumar SG, Devi LG (2011) J Phys Chem A 115:13211
7. Supur M, Fukuzumi S (2002) J Am Chem Soc 124:9582
8. Supur M, Sung YM, Kim D, Fukuzumi S (2013) J Phys Chem C 117:12438
9. Vagnini MT, Smeigh AL, Blakemore JD, Eaton SW, Schley ND, D'Souza F, Crabtree RH, Brudvig GW, Co DT, Wasielewski MR (2012) Proc Natl Acad Sci U S A 109:15651
10. Bottari G, De la Torre G, Guldi DM, Torres T (2010) Chem Rev 110:6768
11. Verma S, Ghosh HN (2012) J Phys Chem Lett 3:1877
12. Supur M, Fukuzumi S (2013) Phys Chem Chem Phys 15:2539
13. Supur M, Fukuzumi S (2012) J Phys Chem C 116:23274

14. Fukuzumi S, Amasaki I, Ohkubo K, Gros CP, Guilard R, Barbe JM (2012) RSC Adv 2:3741
15. Lefler KM, Co DT, Wasielewski MR (2012) J Phys Chem Lett 3: 3798
16. Faul CFJ, Antonietti M (2003) Adv Mater 15:673
17. Newman CR, Frisbie CD, da Silva Filho DA, Brédas JL, Ewbank PC, Mann KR (2004) Chem Mater 16:4436
18. Law KY (1993) Chem Rev 93:449
19. Würthner F (2004) Chem Commun 14:1564
20. Supur M, Fukuzumi S (2013) ECS J Solid State Sci Technol 2: M3051
21. Whitten DG (1993) Acc Chem Res 26:502
22. Martin S, Haiss W, Higgins SJ, Nichols RJ (2010) Nano Lett 10: 2019
23. Dawson RE, Lincoln SF, Easton CJ (2008) Chem Commun 34: 3980
24. Bauer CA, Timofeeva TV, Settersten TB, Patterson BD, Liu V, Simmons BA, Allendorf MD (2007) J Am Chem Soc 129:7136
25. Kole GK, Tan GK, Vittal JJ (2011) CrystEngComm 13:3138
26. Birch DJS, Birks JB (1976) Chem Phys Lett 38:432
27. Greene BI, Hochstrasser RM, Weisman RB (1979) Chem Phys Lett 62:427
28. Waldeck DH (1991) Chem Rev 91:415
29. Hazai L, Hornyak G (1998) ACH-Models Chem 135:493
30. Paci B, Schmidt C, Fiorini C, Nunzi JM, Arbez-Gindre C, Screttas CG (1999) J Chem Phys 111:7486
31. Li Y, Song D (2011) CrystEngComm 13:1821
32. Ma Y, Cheng A, Zhang J, Yue Q, Gao E (2009) Cryst Growth Des 9:867
33. Russ B, Robb MJ, Brunetti FG, Miller PL, Perry EE, Patel SN, Ho V, Chang W, Urban JJ, Chabinyc ML, Hawker CJ, Segalman RA (2014) Adv Mater 26:3473
34. Driscoll PF, Purohit N, Wanichacheva N, Lambert CR, McGimpsey WG (2007) Langmuir 23:13181
35. Quenneville J (1996) Ph.D. Thesis, University of Massachusetts at Amherst
36. Eisfeld A, Briggs JS (2006) Chem Phys 324:376
37. Huang Y, Quan B, Wei Z, Liu G, Sun L (2009) J Phys Chem C 113: 3929
38. Ahrens MJ, Sinks LE, Rybtchinski B, Liu W, Jones BA, Giaimo JM, Gusev AV, Goshe AJ, Tiede DM, Wasielewski MR (2004) J Am Chem Soc 126:8284
39. Weller A (1982) Z Phys Chem 133:93
40. Arnold BR, Farid S, Goodman JL, Gould IR (1996) J Am Chem Soc 118:5482
41. Liao L, Li Y, Zhang X, Geng Y, Zhang J, Xie J, Zeng Q, Wang C (2014) J Phys Chem C 118:15963
42. Supur M, Yamada Y, El-Khouly ME, Honda T, Fukuzumi S (2011) J Phys Chem C 115:15040
43. Idé J, Méreau R, Ducasse L, Castet F (2011) J Phys Chem B 115: 5593
44. Geng Y, Li H, Wu S, Su Z (2012) J Mater Chem 22:20840
45. Pan B, Xing B, Liu W, Xing G, Tao S (2007) Chemosphere 69:1555
46. Han W, Lovell T, Liu T, Noodleman L (2002) ChemPhysChem 3: 167